JMJ24 targets CHROMOMETHYLASE3 for proteasomal degradation in *Arabidopsis*

Shulin Deng,[1] In-Cheol Jang,[1,2] Linlin Su,[1,3] Jun Xu,[1] and Nam-Hai Chua[1]

[1]Laboratory of Plant Molecular Biology, Rockefeller University, New York, New York 10065, USA; [2]Temasek Life Sciences Laboratory, National University of Singapore, 117604 Singapore

H3K9 methylation is usually associated with DNA methylation, and together they symbolize transcriptionally silenced heterochromatin. A number of proteins involved in epigenetic processes have been characterized. However, how the stability of these proteins is regulated at the post-translational level is largely unknown. Here, we show that an *Arabidopsis* JmjC domain protein, JMJ24, possesses ubiquitin E3 ligase activity. JMJ24 directly targets a DNA methyltransferase, CHROMOMETHYLASE 3 (CMT3), for proteasomal degradation to initiate destabilization of the heterochromatic state of endogenous silenced loci. Our results uncover an additional connection between two conserved epigenetic modifications: histone modification and DNA methylation.

Supplemental material is available for this article.

Received November 9, 2015; revised version accepted December 18, 2015.

Methylation of DNA and of H3K9 (H3K9me) are two conserved epigenetic modifications generally associated with gene silencing in eukaryotes. DNA methylation, which is established by DNA methyltransferase 3 (DNMT3) and maintained by the maintenance methyltransferase DNMT1, occurs almost exclusively in the symmetric CG context in mammals. In contrast, in plants, cytosines in all classes of sequence context (that is, CG, CHG, and CHH, where H = A, C, or T) can be methylated (Law and Jacobsen 2010). After DNA methylation has been set up by DOMAINS REARRANGED METHYLTRANSFERASE 2 (DRM2), the methylation states are maintained by three separate pathways in *Arabidopsis*: CG methylation is maintained by the plant homolog of DNMT1, MET1; CHG methylation is maintained by a plant-specific DNA methyltransferase, CHROMOMETHYLASE 3 (CMT3); and the de novo methyltransferase DRM2 is consistently required for the maintenance of asymmetric CHH methylation (Cao et al. 2003; Law and Jacobsen 2010). Recently, CMT2 has been reported to be responsible for the establishment and maintenance of a subset of CHH methylation independently of an RNA-directed DNA methylation pathway (Zemach et al. 2013).

DNA methylation is usually coupled with an increase in H3K9me levels to enforce the transcriptional silencing in both animals and plants (Johnson et al. 2007; Bernatavichute et al. 2008; Du et al. 2015). In *Arabidopsis*, the CHG methylation is highly correlated with H3K9me2 (Bernatavichute et al. 2008; Du et al. 2012) owing to the establishment of a self-reinforcing loop between these two epigenetic marks. CMT3 is recruited by H3K9me2, which is deposited by KRYPTONITE (KYP) to methylate CHG; in turn, methylated CHG DNA recruits KYP to maintain H3K9me2 levels (Johnson et al. 2007; Law and Jacobsen 2010; Du et al. 2012). Histone methylation, including H3K9me, can be reversed by a JmjC domain-containing family of proteins (Klose et al. 2006). Genes encoding 21 JmjC proteins have been identified in *Arabidopsis*, and several proteins have been characterized as active histone demethylases (Lu et al. 2008; Luo et al. 2014).

Transposable elements and repetitive sequences, which are major targets of DNA methylation and H3K9me, are maintained as transcriptionally silenced heterochromatin. Paradoxically, transcription from the silenced loci is required to initiate heterochromatin formation, and the regulation of this process is largely unclear (Grewal and Elgin 2007; Matzke and Mosher 2014; Holoch and Moazed 2015). In fission yeast, a JmjC protein, Epe1, functions specifically to promote the transcription of silenced loci to dynamically maintain heterochromatin (Ayoub et al. 2003; Zofall and Grewal 2006; Trewick et al. 2007). Recently, we reported that JMJ24 functionally resembles Epe1 and plays a conserved role in promoting basal-level transcription of silenced loci to reinforce the RNA-based silencing in *Arabidopsis* (Deng et al. 2015). However, the molecular mechanism of Epe1 and JMJ24 to counteract H3K9me is still unknown, since both proteins harbor an atypical JmjC domain whose demethylase activity is unclear (Klose et al. 2006; Zofall and Grewal 2006; Baba et al. 2011; Deng et al. 2015). Epe1 was assumed to be a protein hydroxylase that affects the stability of a heterochromatin protein, such as Swi6 or Clr4 methyltransferase, thereby regulating the extent and stability of heterochromatin domains (Trewick et al. 2007). *Arabidopsis* JMJ24 harbors a RING motif, and we found that this protein has E3 ubiquitin ligase activity. We also demonstrated that JMJ24 ubiquitinated CMT3 in vitro and destabilized it in vivo. JMJ24 decondenses heterochromatin probably through degradation of CMT3.

Results and Discussion

JMJ24 is an E3 ubiquitin ligase

In addition to the JmjC domain, JMJ24 harbors a RING motif and a coiled-coil (CC) domain (Fig. 1A). As RING

[*Keywords*: CMT3; E3 ligase; histone demethylation; JmjC protein; protein stability; transcriptional gene silencing]

[3]**Present address: Department of Burns and Cutaneous Surgery, Xijing Hospital, Fourth Military Medical University, Xi'an, Shaanxi 710032, China.**

Corresponding author: chua@mail.rockefeller.edu

Article published online ahead of print. Article and publication date are online at http://www.genesdev.org/cgi/doi/10.1101/gad.274647.115.

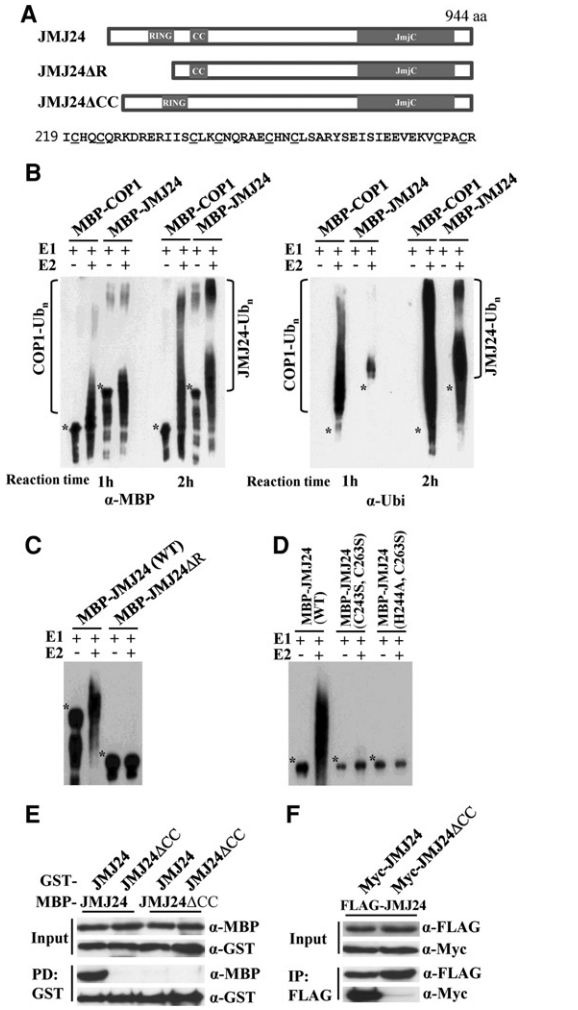

Figure 1. E3 ligase activity of JMJ24. (*A*) Domain organization of wild-type (WT) and truncated derivatives of JMJ24. The *bottom* panel shows the RING motif with conserved cysteine/histidine resides highlighted by underlines. (*B*) MBP-JMJ24 was assayed for E3 activity in the presence or absence of E2. MBP-COP1 was used as a control. The *left* panel was detected by a MBP antibody, and the *right* panel was detected by a ubiquitin antibody. Asterisks indicate the positions of unmodified proteins. (*C*,*D*) MBP-JMJ24 E3 activity is dependent on its RING motif. Wild-type MBP-JMJ24 and RING domain deletion in MBP-JMJ24 (MBP-JMJ24ΔR) (*C*) or two RING motif mutated forms [MBP-JMJ24, MBP-JMJ24(C243S, C263S) and MBP-JMJ24(H244A, C263S)] (*D*) were assayed for self-ubiquitination. Western blots were detected by MBP antibody. (*E*,*F*) Dimerization of JMJ24 in vitro (*E*) and in vivo (*F*). Self-interaction of JMJ24 was examined with wild-type and CC domain deletion (ΔCC) JMJ24 proteins by in vitro assays (*E*) or in plants (*F*). (PD) Pull-down; (IP) immunoprecipitation.

finger proteins are known to have ubiquitin E3 ligase activity (Joazeiro et al. 1999; Lorick et al. 1999; Xie et al. 2002), we examined whether JMJ24 has this activity in vitro. Figure 1B shows that a purified MBP (maltose-binding protein)-JMJ24 fusion protein was able to self-ubiquitinate, whereas JMJ25/IBM1, a close relative of JMJ24, was inactive (Supplemental Fig. S1). The E3 ligase activity of the JMJ24 was abolished when the RING domain was deleted (Fig. 1C). We further constructed two mutant proteins, Cys243 → Ser, Cys263 → Ser(C263S, C263S) and His244 → Ala, Cys263 → Ser(H244A, C263S), in which the RING motif was disrupted. In vitro ubiquitination assays showed that neither mutant protein possessed self-ubiquitination activity (Fig. 1D), suggesting that an intact RING domain is necessary for E3 activity of JMJ24. This is consistent with results obtained from other RING E3 ligases (Xie et al. 2002; Seo et al. 2003). Dimerization is known to activate RING E3 ligase activity, and the CC domain can function to mediate protein dimerization (Lupas 1996; Xie et al. 2002; Seo et al. 2003). To examine the role of the CC domain in JMJ24 dimerization, we expressed MBP and glutathione-S-transferase (GST) fused to wild-type JMJ24 (MBP-JMJ24 and GST-JMJ24) and CC domain-deleted JMJ24 (MPB-JMJ24ΔCC and GST-JMJ24ΔCC) in *Escherichia coli*. Figure 1E shows that JMJ24 can form dimers through the CC domain in vitro. We further confirmed that JMJ24 formed dimers in vivo by coimmunoprecipitation assay using Flag- or Myc-tagged proteins from plant extracts (Fig. 1F). Collectively, these results indicated that JMJ24 possesses properties typical of the RING E3 ligase.

JMJ24 ubiquitinates CMT3 in vitro

The E3 ligase activity of JMJ24 prompted us to hypothesize that JMJ24 may target components involved in heterochromatin formation for degradation. To examine this possibility, we performed a screen and found that JMJ24 interacted with CMT3 in yeast cells (Supplemental Fig. S2; Fig. 2A). Using purified proteins, we confirmed by

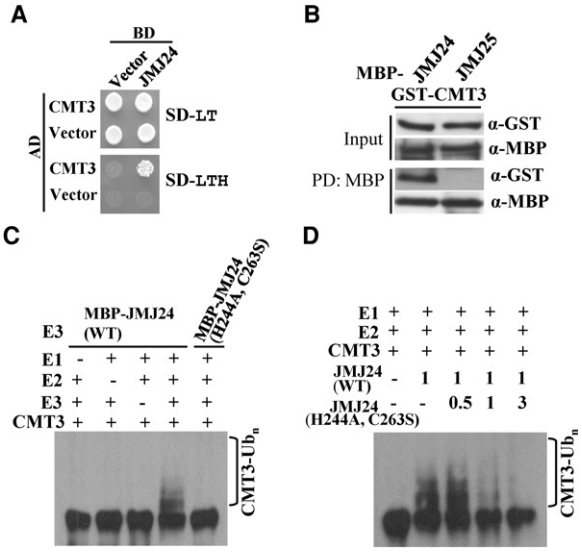

Figure 2. JMJ24 interacts with and ubiquitinates CMT3 in vitro. (*A*) Interaction between the JMJ24 and CMT3 proteins in yeast. SD-LT medium was used for selection of bait and prey proteins. SD-LTH medium was used for selection of bait and prey protein interactions. (*B*) CMT3 physically associates with JMJ24 but not JMJ25/IBM1. Amylose resin was used to pull down (PD) in vitro purified MBP-JMJ24 and MBP-JMJ25, and GST-CMT3 was detected by anti-GST antibody. (*C*) Ubiquitination of CMT3 by JMJ24. GST-CMT3 was polyubiquitinated by wild-type JMJ24 but not RING motif mutated JMJ24 [JMJ24 (H244A, C263S)] in the presence of E1 and E2. (*D*) Ubiquitination of CMT3 by JMJ24 was inhibited by JMJ24(H244A, C263S). The numbers indicate the relative amount of proteins present in the ubiquitination reaction, where 1 equals 500 ng of MBP-fused proteins. (*C*,*D*) Ubiquitination of GST-CMT3 was analyzed using an antibody against GST.

pull-down assays the direct association of JMJ24 with CMT3, but no interaction was seen between JMJ25/IBM1 and CMT3 (Fig. 2B), although the latter protein pair was reported to function in the same genetic pathway (Saze et al. 2008). We further examined whether CMT3 was a target of JMJ24 E3 ligase by in vitro ubiquitination assays. Indeed, CMT3 protein was uibiquitinated by wild-type JMJ24 but not the JMJ24(H244A, C263S) mutant in the presence of E1 and E2 (Fig. 2C). The E3 activity of JMJ24 was inhibited by the RING motif mutant JMJ24 (H244A, C263S) (Fig. 2D), consistent with a previous report that the RING mutant of the E3 ligase can function as a dominant-negative mutant (Xie et al. 2002; Seo et al. 2003).

JMJ24 destabilizes CMT3 in vivo

W next generated double-transgenic plants harboring *35S:Myc-CMT3* and a β-estradiol-inducible (Zuo et al. 2000) *XVE:Flag-JMJ24* to determine whether JMJ24 would associate with CMT3 in vivo. Myc-CMT3, but not Myc-SGS3 (Deng et al. 2015), could be detected in the anti-Flag immunoprecipitates when Flag-JMJ24 was induced, but Myc-CMT3 was not detected in the absence of an inducer (Fig. 3A), indicating a specific association between JMJ24 and CMT3 in vivo. In *Arabidopsis*, Myc-CMT3 levels were reduced when Flag-JMJ24 was transiently overexpressed (Fig. 3B), with no change in *CMT3* mRNA (Supplemental Fig. S3A), indicating that JMJ24 destabilized CMT3 in vivo. In contrast, CMT3 levels were increased upon induction of the dominant-negative mutant of JMJ24, JMJ24(H244A, C263S) (Fig. 3C; Supplemental Fig. S3B). Our results suggest that JMJ24(H244A, C263S) sequestered wild-type JMJ24 and stabilized CMT3. To further confirm that JMJ24 regulates CMT3 stability, we expressed *35S:Myc-CMT3* in wild-type *Arabidopsis* and the *jmj24*-null mutant. CMT3 protein was hardly detected in wild-type without the 26S proteasome inhibitor MG132. However, CMT3 was readily detected in the *jmj24* mutant even without MG132 treatment with similar mRNA expression levels (Fig. 3D). A protein decay experiment showed that the half-life of CMT3 was increased in the *jmj24* mutant compared with the Col-0 wild type (Fig. 3E; Supplemental Fig. S4). Taken together, these results indicate that JMJ24 destabilizes CMT3 in plants.

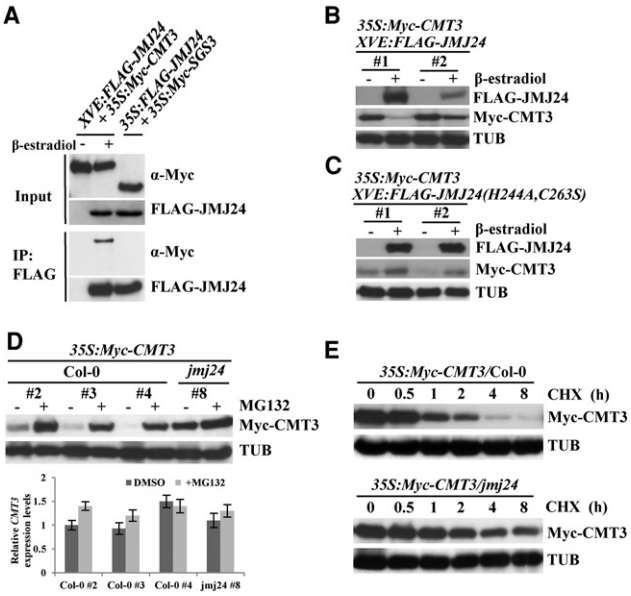

Figure 3. JMJ24 destabilizes CMT3 in vivo. (*A*) JMJ24 associates with CMT3 in vivo. Double-transgenic seedlings carrying *35S:Myc-CMT3* and an estradiol-inducible *XVE:Flag-JMJ24* were treated with (+) or without (−) β-estradiol followed by immunoprecipitation with anti-Flag antibody. Double-transgenic plants carrying Myc-SGS3 and Flag-JMJ24 were used as a control. (*B*,*C*) CMT3 protein levels in response to transient induction (+β-estradiol) of wild-type JMJ24 (*B*) or JMJ24(H244A, C263S) (*C*) in double-transgenic plants. (*D*) CMT3 was stabilized by the 26S proteasome inhibitor MG132. Myc-CMT3 expressed in wild-type or the *jmj24* mutant was analyzed in the presence or absence of MG132 with an antibody against c-Myc. The *bottom* panel shows *CMT3* transcript levels. (*E*) CMT3 protein decay rate in wild-type (*top* panel) or the *jmj24* mutant (*bottom* panel). Samples were treated with cycloheximide (CHX) and collected at the indicated time points for immunoblot analysis using an antibody against c-Myc. Tubulin (TUB) was used a loading control in *B*–*E*.

JMJ24 regulates CHG methylation and H3K9me2 through CMT3

Cytosines in all classes of sequence context (that is, CG, CHG, and CHH, where H = A, C, or T) can be methylated in plants. CMT3 is the main CHG methyltransferase in *Arabidopsis*, and CHG methylation is strongly depleted in *cmt3* mutants (Lindroth et al. 2001; Law and Jacobsen 2010; Stroud et al. 2013). To determine whether JMJ24 regulates CHG methylation on a genome-wide basis, we performed Southern blot analysis with methylation-sensitive enzymes. HpaII and MspI are isoschizomers that recognize 5′-CCGG-3′ sequences with differential sensitivity to methylation. HpaII is inhibited by methylation of either cytosine of the recognition site, whereas MspI is sensitive only to methylation of the outer cytosine and thus detects CHG methylation. Using a highly repetitive Athila retrotransposon long terminal repeat (LTR) as a probe (Lindroth et al. 2001), we found that the Athila LTR showed slight but reproducibly greater resistance to MspI digestion in *jmj24* mutants (Fig. 4A). In contrast, the digestion was increased in *cmt3* mutants (Fig. 4A), consistent with previous reports (Lindroth et al. 2001; Jackson et al. 2002). These results indicate that the CHG methylation increased in *jmj24* but decreased in *cmt3*. The increased CHG methylation in *jmj24* was dependent on CMT3, since the MspI digestion pattern of *jmj24;cmt3* double mutants was identical to *cmt3* single mutants (Fig. 4A). No change of HpaII digestion was detected in either *jmj24* or *cmt3* single mutants or double mutants (Fig. 4A), indicating that neither JMJ24 nor CMT3 had any effect on CG methylation within the Athila LTR. The same results were also detected for two additional loci: 5s-rDNA repeats (Fig. 4B; Supplemental Fig. S5A; He et al. 2009) and centromere satellites (Supplemental Fig. S5B; Vongs et al. 1993). Sequencing of bisulfite-treated DNAs confirmed that the CHG methylation on a representative Athila LTR region (Lindroth et al. 2001) was increased by ~20% in *jmj24* compared with wild-type but was abolished in either the *cmt3* single or *jmj24;cmt3* double mutant (Supplemental Fig. S5C). The direct repeats present on the *FWA* promoter were methylated predominantly at CG sites, leading to the silencing of *FWA* in wild type (Kinoshita et al. 2007). We found the CG and CHH methylation levels remain unchanged, whereas CHG methylation

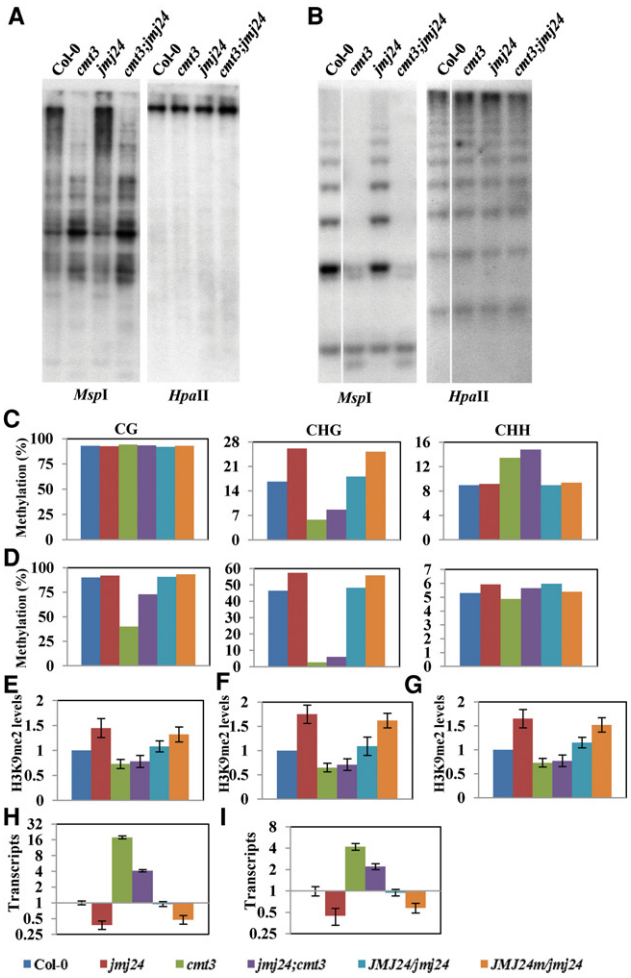

Figure 4. JMJ24 regulates CHG methylation and H3K9me2 through CMT3. (*A*,*B*) Southern blot of MspI- and HpaII-digested genomic DNAs probed with an Athila LTR (*A*) or a 5s rDNA repeat (*B*). See Supplemental Figure S4A for the full scanning of *B*. (*C*,*D*) DNA methylation levels on *FWA* (*C*) and *QQS* (*D*) determined by sequencing of bisulfite-treated genomic DNAs. (*E*–*G*) H3K9me2 accumulation on *FWA* (*E*), *QQS* (*F*), or *SDC* (*G*) promoters in different mutant backgrounds. (*H*,*I*) *QQS* (*H*) and *SDC* (*I*) transcripts levels in different mutant backgrounds. (*jmj24;cmt3*) *jmj24* and *cmt3* double mutant; (*JMJ24/jmj24*) *jmj24* mutant complemented with wild-type JMJ24; (*JMJ24m/jmj24*) *jmj24* mutant complemented with JMJ24(H244A, C263S).

was elevated by ~50% in *jmj24* compared with wild type (Fig. 4C). The CHG methylation was recovered to wild-type levels in *JMJ24/jmj24* in which a wild-type functional JMJ24 was introduced to complement the *jmj24* mutant. However, no recovery of the CHG methylation was seen in *JMJ24m/jmj24* when JMJ24(H244A, C263S) was used for complementation (Fig. 4C; Supplemental Fig. S5D,F). Similar results were also obtained for *QQS* (Fig. 4D; Supplemental Fig. S5E), a de novo protein-coding gene located on the pericentromeric region and regulated epigenetically by both CG and non-CG methylation (Silveira et al. 2013).

CHG methylation colocalizes with H3K9me2, and these two epigenetic marks are interdependent on one another in *Arabidopsis* (Jackson et al. 2002; Law and Jacobsen 2010; Du et al. 2012). Consistent with this, H3K9me2 levels were also increased in promoter regions of *FWA* (Fig. 4E), *QQS* (Fig. 4F), and *SDC* (Fig. 4J) in *jmj24* mutants in accordance with the elevated CHG methylation in the mutants (Fig. 4C,D; Deng et al. 2015). Furthermore, a correlation between the CHG methylation/H3K9me2 and transcripts levels was also observed in these mutants for *QQS* (Fig. 4H) and *SDC* (Fig. 4I), two loci regulated by non-CG methylation. No significant changes for *FWA* transcript levels were detected for all mutants analyzed here (Supplemental Fig. S5G); this is not surprising, as *FWA* is controlled by CG methylation (Lindroth et al. 2001; Kinoshita et al. 2007). Taken together, these results suggest that the RING motif plays an indispensable function for JMJ24, and JMJ24 regulates CHG methylation and H3K9me2 probably through degradation of CMT3.

Post-translational modification plays a critical role in regulating protein activity and stability. The latent H3K9me demethylase activity of a human homolog of Epe1/JMJ24, PHF2, which also harbors an atypical JmjC domain, was stimulated by phosphorylation (Baba et al. 2011). Furthermore, ubiquitin-mediated degradation of DNA-associated proteins adds another regulatory layer to transcriptional regulation, which may be necessary to fine-tune expression patterns in response to environmental signals or developmental cues. Indeed, transcriptional regulators and chromatin-modifying enzymes tend to be unstable (Schwanhausser et al. 2011). The putative H3K9me demethylase Epe1 was rapidly degraded by 26S proteasomes in order to define the proper heterochromatin boundary in yeast (Braun et al. 2011). While it is not clear whether JMJ24 may reveal its demethylase activity after phosphorylation, our results uncover a novel mechanism of the JmjC protein to counteract H3K9me in plants. The RING finger was specifically acquired in the plant clade of JmjC histone demethylase, and this is consistent with the fact that CMT3 is also plant-specific. Our data here present a good example for both conserved (convergent evolution) and diversification mechanisms during evolution.

Materials and methods

DNA construction

The coding sequences of *JMJ24*, *JMJ25/IBM1*, and *CMT3* were PCR-amplified from an *Arabidopsis* cDNA library, digested, and ligased into entry vector *pENTR3C* (Invitrogen). Deletion variants of JMJ24 were generated by overlapping PCR, and point mutation mutants were generated with a QuickChange site-directed mutagenesis kit (Stratagene). Entry vectors were recombined into *pGEX-DC* and *pMAL-DC* for *E. coli* expression or *pBA-DC* (35S promoter) and *pER-DC* (XVE-inducible promoter) for plant expression (Zhang et al. 2005). The *JMJ24m* complementation vector was generated with a QuickChange site-directed mutagenesis kit (Stratagene) from a previous wild-type complementation construct (Deng et al. 2015). Primers are listed in Supplemental Table S1.

Plant material and growth conditions

All *Arabidopsis* used here were in the Col-0 background. The *jmj24* and *cmt3* mutants have been reported: *jmj24-1* (GK-085H03) (Deng et al. 2015) and *cmt3-11* (SALK_148381) (Chan et al. 2006). The *jmj24;cmt3* double mutant was generated by genetic crossing with single mutants. Transgenic plants were generated by the floral dip transformation method (Clough and Bent 1998). Seeds were sterilized and grown on half-strength Murashige-Skoog (MS) medium for 2 wk before being transferred to soil. Plants were grown in a growth chamber at 22°C under 16-h light/8-h dark long-day photoperiod cycles.

Yeast two-hybrid assays

The Matchmaker GAL4-based two-hybrid system (Clontech) was used to perform yeast two-hybrid assays. The full-length JMJ24 coding sequence was inserted into the pGBT9-GW vector (Clontech) to generate a binding domain (BD) JMJ24 fusion (BD-JMJ24) construct. Coding sequences of H3K9 methyltransferases (SUVHs and SUVRs) and DNMTs (Supplemental Fig. S2) were introduced into the pGAD424-GW vector (Clontech) to generate activation domain (AD) fusion constructs. Interactions between AD and BD fusions were assayed according to the manufacturer's instruction.

Protein preparation, in vitro pull-down, and ubiquitination assays

The *E. coli* BL21 strain was used as a host for protein production. Recombinant proteins were purified using amylose resin (New England Biolabs) or glutathione-Sepharose 4 fast flow (GE Healthcare) according to the manufacturer's instructions. Interactions between fusion proteins were determined by pull-down as previously described (Jang et al. 2010). In vitro ubiquitination assays were performed as previously described (Xie et al. 2002; Jang et al. 2010). Each reaction mixture (30 µL) contained 100 ng of rabbit E1 (Boston Biochem), 100 ng of human E2 UbcH5b (Boston Biochem), 2 µg of ubiquitin (Sigma-Aldrich), and 500 ng of E3 (MBP-JMJ24) with or without 500 ng of substrate CMT3. Reactions were incubated for 1 or 2 h at 30°C followed by immunoblot detection.

In vivo coimmunoprecipitation

Two-week-old seedlings of *Flag-JMJ24/Myc-JMJ24*, *Flag-JMJ24/Myc-jmj24ΔCC*, *Flag-JMJ24/Myc-SGS3*, or *XVE:Flag-JMJ24/35S:Myc-CMT3* (treated with or without β-estradiol for 16 h) were ground in liquid nitrogen and homogenized in immunoprecipitation buffer (50 mM Tris-HCl at pH 7.5, 100 mM NaCl, 0.2% Triton X-100, 1 mM DTT, 50 µM MG132, proteinase inhibitor cocktail [Roche]). After centrifugation, supernatants were taken for immunoprecipitation by anti-Flag M2 antibody (Sigma-Aldrich). Antigen–antibody complexes were harvested by protein G agarose beads (Santa Cruz Biotechnology) and washed five times with immunoprecipitation buffer. After being released from agarose beads by boiling for 5 min at 95°C in 2× NuPAGE LDS sample buffer (Life Technologies), proteins in the immunoprecipitates were analyzed by Western blot.

MG132 and cycloheximide treatment

Myc-CMT3 transgenic seedlings were grown on half-strength MS solid medium for 10 d and then transferred to liquid medium with or without 50 µM MG132 (Sigma-Aldrich) for 12 h. Treated seedlings were collected for RNA and immunoblot analysis. To examine the half-life of *Myc-CMT3*, MG132-treated seedlings were washed five times before being transferred to MS liquid medium containing 100 µM cycloheximide to block de novo protein synthesis. Samples were taken at the indicated time points for immunoblot analysis.

RNA analysis

Total RNA was extracted using Trizol reagent (Invitrogen) following the manufacturer's instructions. RNA was treated with a Turbo DNase kit (Ambion) and cleaned up using an RNeasy minikit (Qiagen). On-column DNA digestion was performed using the RNase-free DNase set (Qiagen) during the purification. cDNA was generated from RNA by using the SuperScript III first strand synthesis system (Invitrogen) according to the manufacturer's instructions. Quantitative PCR was performed as previously described (Deng et al. 2015). Data are presented as mean ± SD ($n = 3$).

DNA methylation analysis

Genomic DNAs were extracted from 2-wk-old seedlings using a DNeasy plant minikit (Qiangen). For Southern blots, 5 µg of genomic DNAs was digested with HpaII or MspI (New England Biolabs) overnight. The digested DNA was loaded onto a 1.2% agrose gel and transferred to Hybond-N^+ membranes (GE Healthcare). The Athila LTR, 5S rDNA repeat, and 180-base-pair (bp) centromere repeat were labeled with α-^{32}PdCTP for Southern hybridization to determine their DNA methylation status. Bisulfite DNA conversion was performed by using 0.5–1 µg of genomic DNAs and an EpiTech bisulfite kit (Qiagen) following the manufacturer's protocol. The purified DNAs were used as a template for PCR amplification, and the product was then cloned into the *pGEM-T* easy vector (Promega). For each sample, at least 15 individual clones were sequenced. All experiments were repeated at least twice using different biological samples.

Chromatin immunoprecipitation (ChIP)

ChIP was conducted as described by Gendrel et al. (2005) with minor modifications. Cross-linked chromatin pellets were resuspended in nucleus lysis buffer and sonicated in a Bioruptor UCD 200 (Diagenode) twice for 10 min at the maximum level. Samples were sonicated for periods of 30 sec with a 30-sec interval in between treatments. H3K9me2 antibody (Milipore, catalog no. 07-441) was used for immunoprecipitation. The purified DNA fragments were analyzed by quantitative PCR as described (Deng et al. 2015). The ChIP signal was first normalized against the input DNA and then to the wild-type value. Data are shown as mean ± SD ($n = 3$).

Acknowledgments

We thank Chua laboratory members for discussions. This work was supported in part by the Cooperative Research Program for Agriculture Science and Technology Development (Project PJ906910), Rural Development Administration, Republic of Korea.

References

Ayoub N, Noma K-i, Isaac S, Kahan T, Grewal SI, Cohen A. 2003. A novel jmjC domain protein modulates heterochromatization in fission yeast. *Mol cell biol* **23:** 4356–4370.

Baba A, Ohtake F, Okuno Y, Yokota K, Okada M, Imai Y, Ni M, Meyer CA, Igarashi K, Kanno J, et al. 2011. PKA-dependent regulation of the histone lysine demethylase complex PHF2-ARID5B. *Nat Cell Biol* **13:** 668–675.

Bernatavichute YV, Zhang X, Cokus S, Pellegrini M, Jacobsen SE. 2008. Genome-wide association of histone H3 lysine nine methylation with CHG DNA methylation in *Arabidopsis thaliana*. *PLoS One* **3:** e3156.

Braun S, Garcia JF, Rowley M, Rougemaille M, Shankar S, Madhani HD. 2011. The Cul4-Ddb1 Cdt2 ubiquitin ligase inhibits invasion of a boundary-associated antisilencing factor into heterochromatin. *Cell* **144:** 41–54.

Cao X, Aufsatz W, Zilberman D, Mette MF, Huang MS, Matzke M, Jacobsen SE. 2003. Role of the DRM and CMT3 methyltransferases in RNA-directed DNA methylation. *Curr Biol* **13:** 2212–2217.

Chan SW, Henderson IR, Zhang X, Shah G, Chien JS, Jacobsen SE. 2006. RNAi, DRD1, and histone methylation actively target developmentally important non-CG DNA methylation in *Arabidopsis*. *PLoS Genet* **2:** e83.

Clough SJ, Bent AF. 1998. Floral dip: a simplified method for Agrobacterium-mediated transformation of *Arabidopsis thaliana*. *Plant J* **16:** 735–743.

Deng S, Xu J, Liu J, Kim S-H, Shi S, Chua N-H. 2015. JMJ24 binds to RDR2 and is required for the basal level transcription of silenced loci in *Arabidopsis*. *Plant J* **83:** 770–782.

Du J, Zhong X, Bernatavichute YV, Stroud H, Feng S, Caro E, Vashisht AA, Terragni J, Chin HG, Tu A. 2012. Dual binding of chromomethylase domains to H3K9me2-containing nucleosomes directs DNA methylation in plants. *Cell* **151:** 167–180.

Du J, Johnson LM, Jacobsen SE, Patel DJ. 2015. DNA methylation pathways and their crosstalk with histone methylation. *Nat Rev Mol Cell Biol* **16:** 519–532.

Gendrel A-V, Lippman Z, Martienssen R, Colot V. 2005. Profiling histone modification patterns in plants using genomic tiling microarrays. *Nat Methods* **2:** 213–218.

Grewal SIS, Elgin SCR. 2007. Transcription and RNA interference in the formation of heterochromatin. *Nature* **447:** 399–406.

He X-J, Hsu Y-F, Pontes O, Zhu J, Lu J, Bressan RA, Pikaard C, Wang C-S, Zhu J-K. 2009. NRPD4, a protein related to the RPB4 subunit of RNA polymerase II, is a component of RNA polymerases IV and V and is required for RNA-directed DNA methylation. *Genes Dev* **23:** 318–330.

Holoch D, Moazed D. 2015. RNA-mediated epigenetic regulation of gene expression. *Nat Rev Genet* **16:** 71–84.

Jackson JP, Lindroth AM, Cao X, Jacobsen SE. 2002. Control of CpNpG DNA methylation by the KRYPTONITE histone H3 methyltransferase. *Nature* **416:** 556–560.

Jang I-C, Henriques R, Seo HS, Nagatani A, Chua N-H. 2010. *Arabidopsis* PHYTOCHROME INTERACTING FACTOR proteins promote phytochrome B polyubiquitination by COP1 E3 ligase in the nucleus. *Plant Cell* **22:** 2370–2383.

Joazeiro CAP, Wing SS, Huang H-k, Leverson JD, Hunter T, Liu Y-C. 1999. The tyrosine kinase negative regulator c-Cbl as a RING-Type, E2-dependent ubiquitin-protein ligase. *Science* **286:** 309–312.

Johnson LM, Bostick M, Zhang X, Kraft E, Henderson I, Callis J, Jacobsen SE. 2007. The SRA methyl-cytosine-binding domain links DNA and histone methylation. *Curr Biol* **17:** 379–384.

Kinoshita Y, Saze H, Kinoshita T, Miura A, Soppe WJJ, Koornneef M, Kakutani T. 2007. Control of FWA gene silencing in *Arabidopsis thaliana* by SINE-related direct repeats. *Plant J* **49:** 38–45.

Klose RJ, Kallin EM, Zhang Y. 2006. JmjC-domain-containing proteins and histone demethylation. *Nat Rev Genet* **7:** 715–727.

Law JA, Jacobsen SE. 2010. Establishing, maintaining and modifying DNA methylation patterns in plants and animals. *Nat Rev Genet* **11:** 204–220.

Lindroth AM, Cao X, Jackson JP, Zilberman D, McCallum CM, Henikoff S, Jacobsen SE. 2001. Requirement of CHROMOMETHYLASE3 for maintenance of CpXpG methylation. *Science* **292:** 2077–2080.

Lorick KL, Jensen JP, Fang S, Ong AM, Hatakeyama S, Weissman AM. 1999. RING fingers mediate ubiquitin-conjugating enzyme (E2)-dependent ubiquitination. *Proc Natl Acad Sci* **96:** 11364–11369.

Lu F, Li G, Cui X, Liu C, Wang XJ, Cao X. 2008. Comparative analysis of JmjC domain-containing proteins reveals the potential histone demethylases in *Arabidopsis* and rice. *J Integr Plant Biol* **50:** 886–896.

Luo M, Hung F-Y, Yang S, Liu X, Wu K. 2014. Histone lysine demethylases and their functions in plants. *Plant Mol Biol Rep* **32:** 558–565.

Lupas A. 1996. Coiled coils: new structures and new functions. *Trends Biochem Sci* **21:** 375–382.

Matzke MA, Mosher RA. 2014. RNA-directed DNA methylation: an epigenetic pathway of increasing complexity. *Nat Rev Genet* **15:** 394–408.

Saze H, Shiraishi A, Miura A, Kakutani T. 2008. Control of genic DNA methylation by a jmjC domain-containing protein in *Arabidopsis thaliana*. *Science* **319:** 462–465.

Schwanhausser B, Busse D, Li N, Dittmar G, Schuchhardt J, Wolf J, Chen W, Selbach M. 2011. Global quantification of mammalian gene expression control. *Nature* **473:** 337–342.

Seo HS, Yang J-Y, Ishikawa M, Bolle C, Ballesteros ML, Chua N-H. 2003. LAF1 ubiquitination by COP1 controls photomorphogenesis and is stimulated by SPA1. *Nature* **423:** 995–999.

Silveira AB, Trontin C, Cortijo S, Barau J, Del Bem L, Loudet O, Colot V, Vincentz M. 2013. Extensive natural epigenetic variation at a de novo originated gene. *PLoS Genet* **9:** e1003437.

Stroud H, Greenberg MV, Feng S, Bernatavichute YV, Jacobsen SE. 2013. Comprehensive analysis of silencing mutants reveals complex regulation of the *Arabidopsis* methylome. *Cell* **152:** 352–364.

Trewick SC, Minc E, Antonelli R, Urano T, Allshire RC. 2007. The JmjC domain protein Epe1 prevents unregulated assembly and disassembly of heterochromatin. *EMBO J* **26:** 4670–4682.

Vongs A, Kakutani T, Martienssen R, Richards E. 1993. *Arabidopsis thaliana* DNA methylation mutants. *Science* **260:** 1926–1928.

Xie Q, Guo H-S, Dallman G, Fang S, Weissman AM, Chua N-H. 2002. SINAT5 promotes ubiquitin-related degradation of NAC1 to attenuate auxin signals. *Nature* **419:** 167–170.

Zemach A, Kim MY, Hsieh P-H, Coleman-Derr D, Eshed-Williams L, Thao K, Harmer SL, Zilberman D. 2013. The *Arabidopsis* nucleosome remodeler DDM1 allows DNA methyltransferases to access H1-containing heterochromatin. *Cell* **153:** 193–205.

Zhang X, Garreton V, Chua N-H. 2005. The AIP2 E3 ligase acts as a novel negative regulator of ABA signaling by promoting ABI3 degradation. *Genes Dev* **19:** 1532–1543.

Zofall M, Grewal SI. 2006. Swi6/HP1 recruits a JmjC domain protein to facilitate transcription of heterochromatic repeats. *Mol Cell* **22:** 681–692.

Zuo J, Niu QW, Chua NH. 2000. An estrogen receptor-based transactivator XVE mediates highly inducible gene expression in transgenic plants. *Plant J* **24:** 265–273.